Coastal Engineering 60 (2012) 286–298

Contents lists available at SciVerse ScienceDirect

Coastal Engineering

journal homepage: www.elsevier.com/locate/coastaleng

Empirical design of scour protections around monopile foundations. Part 2: Dynamic approach

Leen De Vos [a,*], Julien De Rouck [a], Peter Troch [a], Peter Frigaard [b]

[a] Ghent University, Dept. of Civil Engineering, Technologiepark 904, 9052 Ghent, Belgium
[b] Aalborg University, Dept. of Civil Engineering, Sohngaardsholmsvej 57, DK-9000 Aalborg, Denmark

ARTICLE INFO

Article history:
Received 11 April 2011
Received in revised form 11 October 2011
Accepted 1 November 2011
Available online 2 December 2011

Keywords:
Monopile
Scour protection
Offshore wind
Design formula
Dynamic stability

ABSTRACT

When building offshore wind turbines, a static scour protection is typically designed, allowing no movement of top layer stones under design conditions, leading to an often conservative design. Furthermore, little design guidelines exist for a scour protection around a monopile foundation under combined wave and current loading.

In part 1 (De Vos et al., 2011), preceding this paper, a static design guideline for a scour protection around a monopile is suggested, based on a combined wave and current flow field. By allowing some movement of the top layer stones of the scour protection, a more economical design is obtained. This paper describes the derivation of a dynamic design formula to calculate the required stone size for a scour protection around a monopile foundation in a combined wave and current climate. The formula is based on the results of an experimental model study, described in this paper. The formula gives an expected damage level to the scour protection, based on the wave orbital velocity, wave period, steady current velocity, water depth, relative stone density and stone size.

When applying the formula for a typical situation in the North Sea, a reduction of 20% to 80% of the required stone size is obtained, compared to the static design approach, described in part 1.

1. Introduction

When designing a statically stable scour protection, in principle no damage to the top layer is accepted. For such a scour protection, damage is defined as the displacement of top layer stones. As the design life time of offshore wind turbines is typically only 20 years (den Boon et al., 2003), it is important to decrease the costs of a wind turbine as much as possible. An opportunity to do this can be found in using significantly smaller rock sizes for the scour protection. The use of smaller rock sizes decreases the basic cost of the protection layer, additionally it may lead a decrease of the cost by reducing the number of filter layers.

When designing a scour protection with smaller elements, allowing movement of individual stones without failure of the protection, it is important:

- to clearly define damage;
- to formulate an acceptable damage criterion;
- to add damage as a parameter in the stability formula;
- to account for damage development over time as an important element in the design of scour protections.

Going even one step further, Van der Meer (1988) investigated breakwaters with smaller stone sizes than ordinarily used for a statically stable design. He came to the conclusion that such breakwaters develop a dynamically stable profile, for breakwater damage as a function of time reaches an equilibrium state (Fig. 1, curve 3). The same could be valid for bottom protections. Fig. 1 (CIRIA/CUR, 1991) shows that damage development for a bottom protection also develops towards an equilibrium state (curve 2). This is in clear contrast with a progressive failure mechanism in which damage increases exponentially. The similar decrease in damage rate for bed protections and breakwaters leads to the expectation that a dynamically stable profile might develop when the stone size of the scour protection is decreased. On this subject, Chiew (1995) investigated the stability of a riprap layer around a cylindrical bridge pier. He found that partial damage of a riprap layer led to rearmouring by the coarse riprap stones, which could effectively prevent a total disintegration of the riprap layer.

In this paper, the design of a dynamically stable scour protection is aspired. For such a scour protection, it is important to know whether the developed profile remains stable or whether damage might accumulate over time and ultimately lead to the scour protection's failure. The present study shows that limited movement of top layer stones is

* Corresponding author.
E-mail addresses: Leen.DeVos@mow.vlaanderen.be (L. De Vos), Julien.Derouck@UGent.be (J. De Rouck), Peter.Troch@UGent.be (P. Troch), pf@civil.aau.dk (P. Frigaard).

0378-3839/$ – see front matter © 2011 Elsevier B.V. All rights reserved.
doi:10.1016/j.coastaleng.2011.11.001

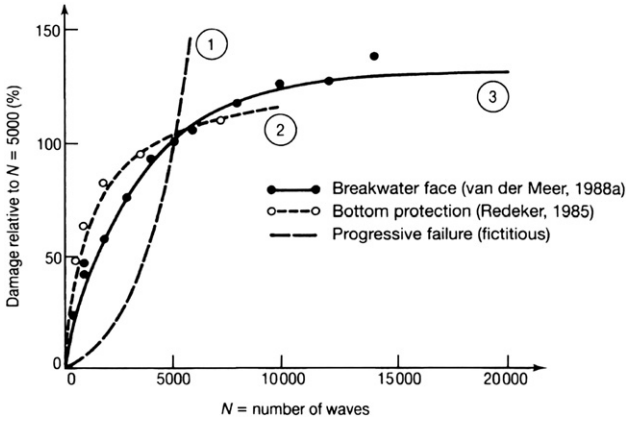

Fig. 1. Damage evolution as a function of time; from CIRIA/CUR (1991), based on Van der Meer (1988) and Redeker (1985).

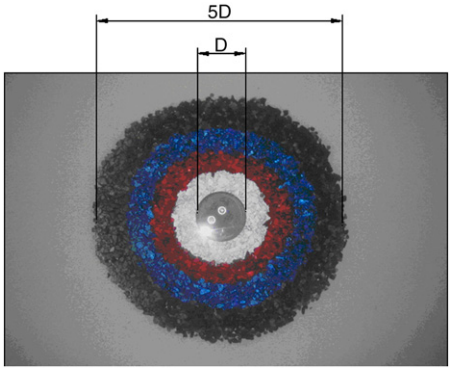

Fig. 2. Top view of a scour protection, before loading (note that the pile was removed to make measurements).

acceptable, without causing failure of the scour protection. A design formula is suggested.

Even for a statically stable scour protection, the present study has an added value. For such a scour protection damage might develop when the design criteria are exceeded. In this case, information on the development of the damage in time and the amount of damage which can be expected is important regarding the maintenance of the scour protection. Exceeding the design criteria for static scour protection can be expected, as a relatively short return period is often used for the design of scour protections. This can be related to the limited life cycle of offshore wind turbines (approximately 20 years) and the fact that a scour protection failure hardly ever leads to potentially lethal situations, or even the failure of the wind turbine's foundation. Typically a return period of 50 years is considered acceptable for static scour protections and chances of encountering higher loads than the design loads are therefore significant. For example, a return period of 50 years and a design lifetime of 20 years lead to an exceedance probability of 33% of the design storm.

In De Vos et al. (2011, part 1 of this paper), a description of the state of the art in scour protection design is given, along with an illustration of the general experimental set-up. In Section 2, a short description of the experimental set-up is given, focussing on the differences from the tests described in part 1. Section 3 emphasises the analysis of the model tests and the derivation of the design formula, whereas Section 4 compares the design formula with the traditional design methods and the formula derived in part 1 preceding this paper.

2. Experimental set-up

2.1. General description of set-up and model

All experiments are carried out in a 1 m wide wave flume at the Department of Civil Engineering of Ghent University. A reference is made to De Vos et al. (2011) for the details of the description of the experimental set-up.

A model of a monopile is built in the middle of the wave flume, centrally in a 4 m long sandbox. The diameter of the monopile is 0.1 m and represents a typical monopile foundation for offshore wind turbines in the North Sea on a scale 1/50. A scour protection made of stones is placed around the monopile foundation, placed on top of a filter. Stones are painted in different colours to allow visual observation of the amount and direction of displacement (Fig. 2). The coloured stones are placed in concentric circles around the pile. Each ring has a width equal to the piles' radius. The overall diameter of the applied scour protection is 5 times the pile diameter. 10% extra material is used for the outer ring, to make sure some material is placed beside the filter without decreasing the height of the outer ring. The thickness of the scour protection is typically $2.5D_{n50}$, but was increased to $3D_{n50}$ for two tests.

For the present study, the sand was flattened before each test and a new scour protection was placed to ensure that the test conditions were equal for each test. The scour protection was installed on top of the sand bed. The sediment size applied for the sand bed was 100 μm (very fine sand).

2.2. Scour protection characteristics

Four different rock armour gradings are used throughout the tests. The gradings which are used are: 2–80 kg, 10–30 kg; 2–300 kg and 80–300 kg (prototype values). The first two gradings yield the same median grain size D_{50}. The resulting median grain sizes D_{50} are 0.205 m, 0.300 m and 0.425 m on prototype scale. A Froude scaling was applied on the grain size of the stones, resulting in model scale values of the median grain size of 4.1 mm (for both 2–80 and 10–30 kg), 6.0 mm and 8.5 mm.

The stones of the scour protection exist of angular rocks. Two different mass densities are used for the scour protection material: $\rho_s = 2650$ kg/m³ and $\rho_s = 3200$ kg/m³. The latter stones are actually steel slag. Steel slag aggregates are highly angular in shape and have rough surface texture. They have high bulk densities and moderate water absorption (Federal Highway Administration, 2008), which makes them ideal as high density stones.

Washing out of fine bed material through the rocks might cause failure of the scour protection. This is avoided by applying a filter layer. For offshore situations it is common to use a single or a double filter layer. However, during the tests a geotextile was mostly used as a filter for the sake of convenience and because the main interest of the experiments is the stability of and the damage to the scour protection layer. To investigate the influence of the filter on the stability of the top layer, two alternatives for the geotextile are considered:

- Scour protection without filter
- Scour protection with a granular filter, with the following characteristics: $d_{f15} = 0.6$ mm, $d_{f50} = 1.5$ mm and $d_{f85} = 1.8$ mm. One filter layer was sufficient and satisfied the filter criteria both for the transition bed material to filter layer and filter layer to top layer, and this for all stone sizes used in the different top layers. The filter layer thickness was 1 cm in model scale and the filter was placed on top of the sand bed.

2.3. Hydraulic conditions

Irregular wave tests are carried out for a range of wave heights and wave periods, combined with different steady current velocities following or opposing the waves. Two different water depths are used throughout the tests. For each test, characterised by a combination

Table 1
Experimental conditions for dynamic stability tests (measured characteristics).

Test no [−]	N [−]	d [m]	D_{n50} [mm]	s [−]	U_c [m/s]	H_{m0} [m]	T_p [s]	Filter [−]	t_s [times D_{n50}]	D_{85}/D_{15} [−]
1	5000	0.4	3.5	2.65	0	0.139	1.45	Geotextile	2.5	2.48
2	5000	0.4	3.5	2.65	0	0.125	1.71	Geotextile	2.5	2.48
3	5000	0.4	3.5	2.65	0	0.141	1.71	Geotextile	2.5	2.48
4	5000	0.4	3.5	2.65	0	0.156	1.71	Geotextile	2.5	2.48
5	5000	0.4	3.5	2.65	0.077	0.120	1.16	Geotextile	2.5	2.48
6	5000	0.4	3.5	2.65	0.080	0.135	1.42	Geotextile	2.5	2.48
7	5000	0.4	3.5	2.65	0.077	0.120	1.71	Geotextile	2.5	2.48
8	5000	0.4	3.5	2.65	0.081	0.136	1.71	Geotextile	2.5	2.48
10	0	0.4	3.5	2.65	0.140	-	-	Geotextile	2.5	2.48
11	5000	0.4	3.5	2.65	0.164	0.118	1.20	Geotextile	2.5	2.48
12	1000	0.4	3.5	2.65	0.147	0.050	1.42	Geotextile	2.5	2.48
13	3000	0.4	3.5	2.65	0.150	0.069	1.42	Geotextile	2.5	2.48
14	5000	0.4	3.5	2.65	0.164	0.088	1.42	Geotextile	2.5	2.48
15	5000	0.4	3.5	2.65	0.159	0.114	1.42	Geotextile	2.5	2.48
15*	5000	0.4	3.5	2.65	0.167	0.114	1.42	Geotextile	2.5	2.48
15**	5000	0.4	3.5	2.65	0.167	0.114	1.42	Geotextile	2.5	2.48
16	5000	0.4	3.5	2.65	0.165	0.129	1.42	Geotextile	2.5	2.48
17	5000	0.4	3.5	2.65	0.161	0.140	1.40	Geotextile	2.5	2.48
18	5000	0.4	3.5	2.65	0.164	0.115	1.71	Geotextile	2.5	2.48
19	5000	0.4	3.5	2.65	0.163	0.130	1.71	Geotextile	2.5	2.48
20	3000	0.4	3.5	2.65	0.160	0.145	1.71	Geotextile	2.5	2.48
20*	5000	0.4	3.5	2.65	0.167	0.145	1.71	Geotextile	2.5	2.48
20**	5000	0.4	3.5	2.65	0.159	0.145	1.71	Geotextile	2.5	2.48
21	0	0.4	3.5	2.65	0.205	-	-	Geotextile	2.5	2.48
22	3000	0.4	3.5	2.65	0.230	0.083	1.42	Geotextile	2.5	2.48
23	0	0.4	3.5	2.65	0.253	-	-	Geotextile	2.5	2.48
24	5000	0.4	3.5	2.65	−0.067	0.146	1.71	Geotextile	2.5	2.48
25	5000	0.4	3.5	2.65	−0.142	0.099	1.42	Geotextile	2.5	2.48
26	5000	0.4	3.5	2.65	−0.138	0.117	1.42	Geotextile	2.5	2.48
27	5000	0.4	3.5	2.65	−0.137	0.134	1.37	Geotextile	2.5	2.48
28	5000	0.4	3.5	2.65	0	0.139	1.45	Geotextile	2.5	1.32
29	5000	0.4	3.5	2.65	0	0.141	1.71	Geotextile	2.5	1.32
30	5000	0.4	3.5	2.65	0	0.156	1.71	Geotextile	2.5	1.32
31	5000	0.4	3.5	2.65	0.166	0.114	1.42	Geotextile	2.5	1.32
32	5000	0.4	3.5	2.65	0.164	0.115	1.71	Geotextile	2.5	1.32
33	3000	0.4	3.5	2.65	0.161	0.145	1.71	Geotextile	2.5	1.32
34	5000	0.4	3.5	2.65	0.212	0.083	1.42	Geotextile	2.5	1.32
35	3000	0.4	3.5	2.65	0.233	0.109	1.71	Geotextile	2.5	1.32
36	3000	0.4	3.5	2.65	−0.147	0.134	1.71	Geotextile	2.5	1.32
37	5000	0.4	3.5	2.65	0.154	0.115	1.71	No	2.5	2.48
38	5000 + extra	0.4	3.5	2.65	0.164	0.145	1.71	No	2.5	2.48
38*	5000	0.4	3.5	2.65	0.155	0.145	1.71	No	2.5	2.48
39	5000	0.4	3.5	2.65	0.169	0.115	1.71	No	3	2.48
40	5000	0.4	3.5	2.65	0.156	0.145	1.71	No	3	2.48
41	5000	0.4	3.5	2.65	0.151	0.145	1.71	Granular	2.5	2.48
41a	0	0.2	3.5	2.65	0.317	-	-	Granular	2.5	2.48
42	5000	0.4	3.5	2.65	tidal +0.159 −0.150	0.115	1.71	Geotextile	2.5	2.48
43	3000	0.2	3.5	2.65	0.172	0.080	1.79	Geotextile	2.5	2.48
44	5000	0.4	5	2.65	0	0.156	1.71	Geotextile	2.5	4
45	5000	0.4	5	2.65	0.077	0.152	1.71	Geotextile	2.5	4
46	5000	0.4	5	2.65	0.164	0.129	1.42	Geotextile	2.5	4
47	5000	0.4	5	2.65	0.165	0.140	1.40	Geotextile	2.5	4
48	5000	0.4	5	2.65	0.163	0.130	1.71	Geotextile	2.5	4
49	5000	0.4	5	2.65	0.158	0.145	1.71	Geotextile	2.5	4
50	5000	0.4	5	2.65	0.224	0.109	1.71	Geotextile	2.5	4
51	5000	0.4	5	2.65	0.227	0.140	1.71	Geotextile	2.5	4
52	3000	0.2	5	2.65	0.315	0.058	1.71	Geotextile	2.5	4
53	5000	0.4	7.2	2.65	0.156	0.145	1.71	Geotextile	2.5	1.39
54	5000	0.4	7.2	2.65	0.221	0.121	1.42	Geotextile	2.5	1.39
55	5000	0.4	7.2	2.65	0.221	0.140	1.71	Geotextile	2.5	1.39
56	5000	0.2	7.2	2.65	0.168	0.080	1.79	Geotextile	2.5	1.39
57	3000	0.2	7.2	2.65	0.299	0.086	1.71	Geotextile	2.5	1.39
58	5000	0.4	7.2	2.65	−0.142	0.163	1.71	Geotextile	2.5	1.39
59	5000	0.4	7.2	2.65	0.236	0.140	1.71	No	2.5	1.39
60	5000	0.4	-	-	0.147	-	-	-		scour
61	5000	0.4	-	-	0.203	-	-	-		scour
62	5000	0.2	-	-	0.298	-	-	-		scour
71	3000	0.4	3.5	3.2	0	0.168	1.71	Geotextile	2.5	2.48
72	3000	0.4	3.5	3.2	0	0.155	1.71	Geotextile	2.5	2.48
73	3000	0.4	3.5	3.2	0.066	0.151	1.71	Geotextile	2.5	2.48
74	3000	0.4	3.5	3.2	0.143	0.128	1.42	Geotextile	2.5	2.48
75	3000	0.4	3.5	3.2	0.146	0.139	1.35	Geotextile	2.5	2.48
76	3000	0.4	3.5	3.2	0.141	0.146	1.71	Geotextile	2.5	2.48
77	3000	0.4	3.5	3.2	0.203	0.122	1.42	Geotextile	2.5	2.48
78	3000	0.4	3.5	3.2	0.195	0.107	1.42	Geotextile	2.5	2.48

Table 1 (*continued*)

Test no [−]	N [−]	d [m]	D_{n50} [mm]	s [−]	U_c [m/s]	H_{m0} [m]	T_p [s]	Filter [−]	t_s [times D_{n50}]	D_{85}/D_{15} [−]
81	3000	0.4	5	3.2	0	0.168	1.71	Geotextile	2.5	4
82	3000	0.4	5	3.2	0	0.146	1.71	Geotextile	2.5	4
83	3000	0.4	5	3.2	0.202	0.124	1.71	Geotextile	2.5	4
84	3000	0.4	5	3.2	0.214	0.135	1.42	Geotextile	2.5	4
85	3000	0.4	5	3.2	0.212	0.139	1.71	Geotextile	2.5	4

of the loading parameters, three consecutive wave trains are generated. Generally, an initial wave train of 1000 waves is followed by two wave trains of 2000 waves. When the scour protection has failed after 3000 waves, the second wave train of 2000 waves is not generated.

The complete test program is given in Table 1, depicting the total number of waves N, the water depth d, the nominal stone diameter D_{n50} of the scour protection ($D_{n50} = 0.84D_{50}$), the relative stone density s ($=\rho_s/\rho_w$), the steady current velocity U_c, the significant wave height H_{m0}, the peak wave period T_p, the applied filter, the thickness of the scour protection t_s and the value of D_{85}/D_{15} which characterises the stone's grading. The test numbers marked with an asterisk* and ** are a repetition of the same test. Repetitions were done to check the repeatability of the tests.

The target spectrum of the irregular waves is a JONSWAP spectrum, with a peak enhancement factor $\gamma = 3.3$. The test series were carried out without the monopile in the wave flume and wave characteristics were measured at the location of the pile to determine the undisturbed wave field. A low-reflection absorption beach is installed at the end of the flume, leading to a reflection of approximately 15% of the wave height. This means that reflection is small enough to be neglected (no active wave absorption was used throughout the tests).

When testing different stone sizes, the exact same time series was repeated, to allow comparison of the stone stability under the (as good as possible) exact same environmental conditions.

As 3 successive wave trains are generated for each test, the characteristic values of a test are determined as a weighted average of the wave trains. In Table 1, the characteristics of the first 3000 waves are given, as 3000 waves are used for the main damage analysis. For the wave height H_{m0}, the value after 3000 waves is calculated as:

$$H_{m0} = \frac{1}{3}\left(H_{m0,1000} + 2H_{m0,2000}\right) \quad (1)$$

with $H_{m0,1000}$ the significant wave height of the test series with 1000 waves and $H_{m0,2000}$ the significant wave height of the first test series with 2000 waves. For the wave height after 5000 waves, the same method was used to obtain a weighted average for H_{m0}, by also weighing the measured value of H_{m0} of the second test series with 2000 waves.

The other characteristics (both steady current velocity and wave characteristics) are treated the same way.

2.4. Measurements

In addition to the visual observations of the displaced top layer stones, 3D measurements are made of the scour protection before each test and after each wave series. A remote controlled profiler is used to measure the surface (sand bottom, armour layer) and track changes due to erosion and accretion. The profiler was designed at

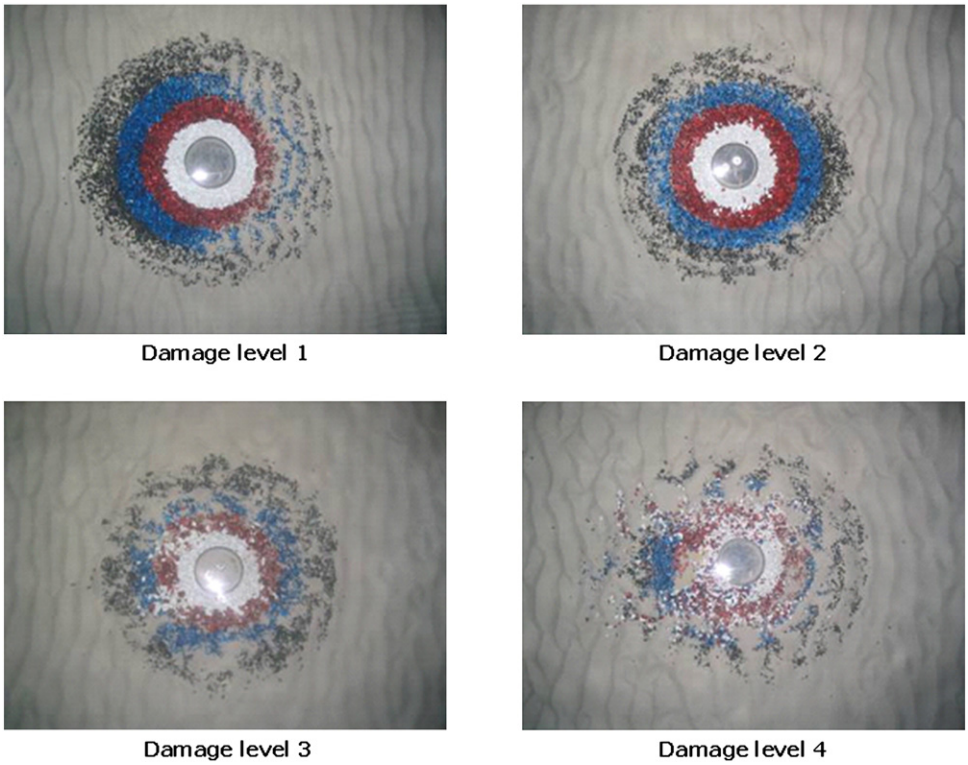

Fig. 3. Example of visual damage levels: damage level 1: no movement of the stones; damage level 2: very limited movement of stones; damage level 3: significant movement of stones, without failure of the protection; damage level 4: failure of the protection.

Aalborg University. The profiler operates in a non-contact manner using a laser to make the measurements and is able to operate even if the target is under water. The profiler has three degrees of freedom: forward/backward; left/right and up/down and each of the axes is controlled by high precision step-motors, capable of a movement resolution less than 0.1 mm, enabling the profiler to position the laser very accurately.

For the present test set-up, the profiler measures a square surface of 0.6 m (width) × 0.7 m (length) around the pile. This surface is overlaid with a grid of 5 mm × 5 mm, which is slightly larger than the smallest value of D_{50} which was tested. Van der Meer (1988) used a comparable grid and measured with steps of 0.04 m for stones with a $D_{n50} = 0.036$ m.

3. Analysis of the experimental model tests

As mentioned earlier, most scour protections are designed according to a static stability criterion, which states that stones have to remain stable under the maximum load. The presented test series is performed to assess which formula could lead to a more economical design by allowing limited movement of top layer stones, without causing failure of the scour protection. Combined irregular wave and current tests were performed and 3D measurements of the scour protection were made to quantify the damage to the scour protection.

3.1. Analysis method

The analysis of the damage is based both on visual observations (top view pictures are taken before each test and after each wave series) and 3D profiler measurements. The pictures of all tests are shown in Appendix A.

3.1.1. Damage definition

For the visual damage analysis, four damage levels are distinguished (Fig. 3):

- damage level 1: no movement of the stones
- damage level 2: very limited movement of stones
- damage level 3: significant movement of stones, without failure of the protection
- damage level 4: failure of the protection

The scour protection is considered to have failed when the filter is exposed over a minimum area of four armour units ($4D_{50}^2$). This is the same failure definition which is used for statically stable scour protections (den Boon et al., 2004).

For the analysis of the profiler measurements, only the area which is covered by the scour protection (ring with outer diameter 5D and inner diameter D) is considered. The scour protection is divided into sub areas to quantify the damage.

The division into sub areas is done as shown in Fig. 4. The scour protection area is divided into 4 rings, corresponding with the 4 coloured rings in the set-up (Fig. 2). Each ring has a width of 0.05 m, corresponding to the radius of the pile. The extra material which is used for the outer ring, is not taken into account for the analysis. The rings are then further divided into different sub areas, with a size equal to the pile's area. The orientation of the zones is chosen to optimally represent

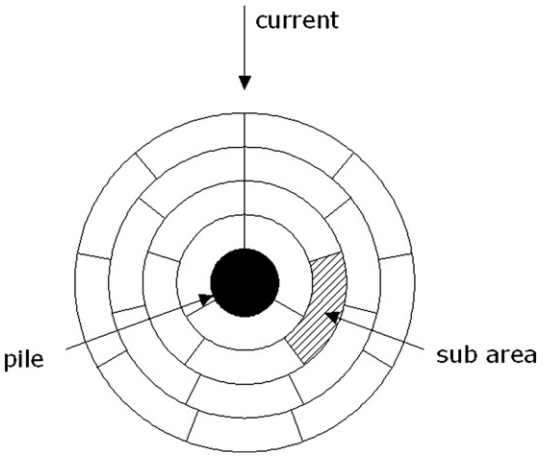

Fig. 4. Division of the scour protection into sub areas.

Table 2
Visual damage and damage number for all irregular wave tests.

Test no [−]	S_{3D} [−]	Visual damage level [−]	Test no [−]	S_{3D} [−]	Visual damage level [−]
1	0.81	3	37	0.73	-
2	0.96	3	38	1.83	4
3	1.21	4	38*	1.66	-
4	1.67	4	39	0.78	-
5	0.11	1	40	1.42	-
6	0.60	3	41	2.19	4
7	0.80	3	43	1.57	4
8	1.12	3	44	0.99	3
11	0.08	1	45	0.88	3
13	0.07	1	46	0.23	1
14	0.24	1	47	0.33	2
15	0.37	2	48	0.49	3
15*	0.31	2	49	0.85	3
15**	0.38	2	50	0.64	3
16	0.73	3	51	1.22	4
17	0.82	3	52	1.21	4
18	1.99	4	53	0.35	2
19	0.94	3	54	0.19	2
20	1.84	4	55	0.58	3
20*	1.53	4	56	0.18	2
20**	1.55	4	58	0.91	3
22	1.28	4	59	0.78	3
24	1.85	4	71	1.57	-
25	0.18	2	72	1.10	-
26	-	4	73	0.98	-
27	1.20	4	74	0.40	-
28	0.72	3	75	0.62	-
29	1.19	4	76	0.98	-
30	1.54	4	77	0.99	-
31	0.14	2	78	0.60	-
32	0.76	3	81	0.73	-
33	1.48	4	82	0.50	-
34	0.44	2	83	0.41	-
35	2.33	4	84	0.40	-
36	2.39	4	85	0.73	-

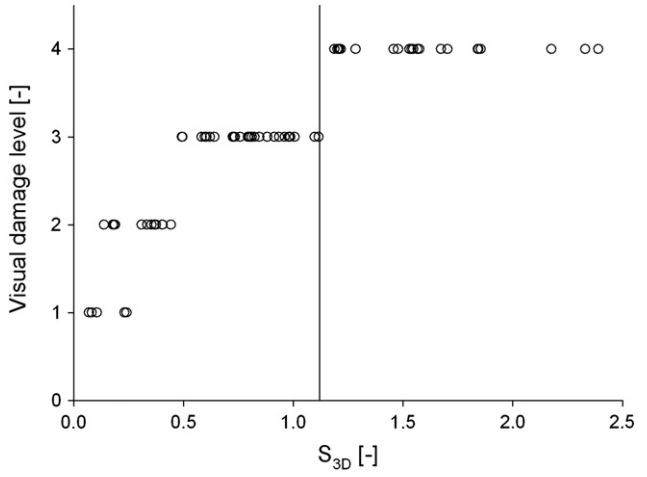

Fig. 5. Visual damage level versus measured damage number. Damage level 1: no movement of the stones; damage level 2: very limited movement of stones; damage level 3: significant movement of stones, without failure of the protection; damage level 4: failure of the protection.

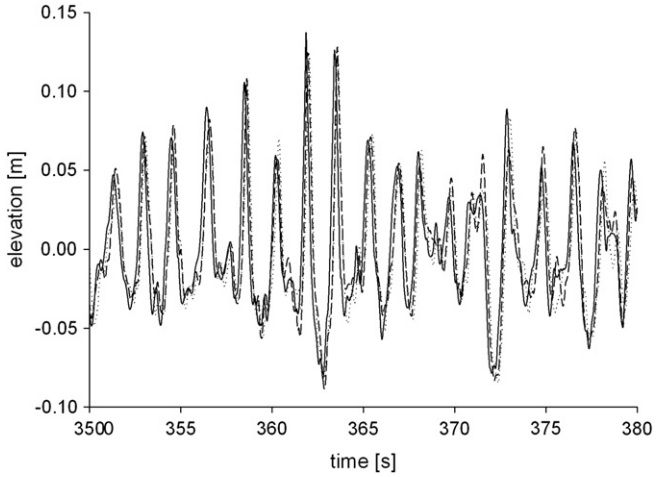

Fig. 6. Fraction of time series elevations for test 15.

the damage location and is therefore mainly based on the current direction: when considering the direction of the current, damage is mainly located down current of the pile (see Section 3.1.4), or at the sides of the pile in the case no current is present.

Dividing the scour protection into different zones with an equal surface area has several advantages. It facilitates the analysis of the results, as the damage can be located. Secondly the resulting damage becomes independent of the radial extent of the scour protection, as it is the sub area with the highest damage which is withheld to define the damage number. Another main advantage is that the accuracy of the damage number is significantly improved by using smaller surfaces with a higher damage number.

When talking about (dynamic) scour protection stability, a clear damage definition is required. Damage after a storm (or test) can be measured by either counting the number of displaced stones, or by comparing the initial profile with the profile after the event. For breakwaters, the two-dimensional damage is quantified by Van der Meer (1988) as $S = A_e/D_{n50}^2$, with A_e the eroded cross-sectional area of the profile and D_{n50} the nominal stone diameter. This implies that the damage S is equal to the number of squares with side D_{n50} which fit into the eroded area A_e. Similar to this definition, the three-dimensional damage of a scour protection could be defined as:

$$S_{3D}^{'} = \frac{V_e}{D_{n50}^3} \tag{2}$$

with V_e the eroded volume, $S_{3D}^{'}$ equals the number of cubes with side D_{n50} which fits into V_e. As the applied stones are small, another definition is used for the quantitative analysis of the damage. The three-dimensional damage number $S_{3D,sub}$ is defined per sub area as the ratio of eroded volume V_e and the surface of the sub area times the stone diameter:

$$S_{3D,sub} = \frac{V_e}{D_{n50} \cdot \pi \frac{D^2}{4}} \tag{3}$$

with D the pile diameter. Eq. (3) represents the average height of stones which has disappeared over the considered sub area, expressed as a function of the nominal stone diameter D_{n50} (when $S_{3D,sub} = 1$, this implies that the height of the scour protection has decreased over this sub area over a distance equal to D_{n50}). The damage is calculated for each sub area (Fig. 4) according to Eq. (3) and the damage number S_{3D} is defined as the highest damage which is obtained by considering all the sub areas:

$$S_{3D} = \max\left(S_{3D,sub}\right) \tag{4}$$

Table 2 shows the visual damage level and the damage number for the different tests after 3000 waves, determined with Eq. (4) and as described earlier. A visual estimate of the damage can only be made when coloured stones are used. For some tests, this was not the case, leading to missing visual damage levels in Table 2. For 1 test (test no 26), the measurement of the initial profile failed and as a result no measured damage number is available for this test. Fig. 5 graphically represents the data in Table 2, showing that there is a clear relationship between visual damage and measured damage number, defined with Eq. (4). With the profiler, it is difficult to measure small damages, leading to an overestimation of the damage number when no movement can be established visually.

3.1.2. Repeatability

When carrying out model tests to develop a prediction formula, repeatability of the tests is of the utmost importance. Both the reproducibility of the loading conditions (waves and current) and of the damage is essential and was verified during the tests. This was done by repeating some tests (once or twice) to get a view of the repeatability of the tests. These were tests 15, 20 and 38 (see Table 1).

In repeating the tests, it was aspired to reproduce the wave characteristics of the tests exactly by using the same time series for the elevations. It was impossible to reproduce the exact same steady flow velocity. Fig. 6 shows part of the measured elevations during test 15, which was performed three times. It shows that the influence of the difference in flow velocity on the wave elevations is limited.

For the reproducibility of the damage, two aspects need to be considered. Both the stone movement due to flow action and the damage

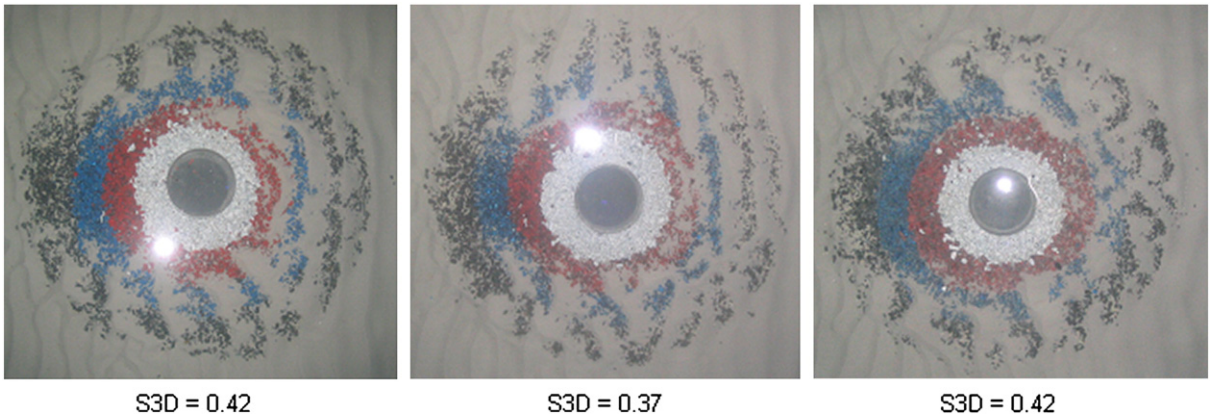

Fig. 7. Damage after 3000 waves for repetitions of test 15; waves and current are travelling from right to left.

measurement should not be prone to large variations. To assess the latter, the profiler measurement of the same situation (test 29, after 1000 waves) was repeated several times. The deviation of the damage number (according to Eq. (4)) is less than 5% of the average for a damage number of 0.9.

Considering the reproducibility of the damage, Figs. 7 and 8 show the pictures of the repeated tests 15 and 20 after 3000 waves. The damage numbers are, for test 15: $S_{3D}=0.42$, 0.37 and 0.42. For test 20, the respective damage numbers are $S_{3D}=1.84$, 1.57 and 1.57.

For test 15, the damage is highly reproducible (visual damage level 2). For test 20 (visual damage level 4), the damage development differs more. All tests do however categorise under damage level 4, as the geotextile filter is clearly visible in all cases. The repeatability of tests with low damage numbers is considered to be better compared to tests with high damage numbers.

3.1.3. Governing parameters

Generally, governing parameters can be classified into parameters related to environmental conditions and parameters related to the structure's characteristics. Tables 3 and 4 list the governing environmental and structural parameters for the test series. In the tables, it is indicated whether the parameters are varied during the tests or not.

For each of the tested parameters, the influence was separately investigated to obtain the result, described in Section 3.2.

3.1.4. Location of damage

Breusers and Raudkivi (1991) and Sumer and Fredsøe (2002) give a clear description of the flow pattern around a single vertical pile. When a vertical pile is placed on a sea bed, the flow experiences the following changes (Fig. 9):

- a downflow is formed in front of the pile
- a horseshoe vortex originates in front of the pile
- a vortex flow pattern is formed at the lee-side of the pile (usually accompanied by vortex shedding)
- the streamlines are contracted at the side edges of the pile

The changes in the flow pattern, described earlier, generally create an increase (1) in the bed shear-stress and (2) in the turbulence level near the structure, both leading to an increase in local sediment transport capacity near the structure and thus scour. They are also the same changes in the flow pattern which induce damage to the scour protection (if we disregard edge effects). Not so much information can be found in the literature on this topic.

For this reason, the location of the damage was investigated to assess whether a distinctive damage profile could be distinguished. It was found that the location of the damage mainly depends on the flow characteristics, leading to the three typical damage profiles shown in Fig. 10, which represent the damage at the scour protection

Table 3
Environmental parameters.

Parameter	Dimension	Description	Variation
U_c	m/s	Average flow velocity	Yes
D	m	Water depth	Yes
H_s	m	Significant wave height	Yes
T_p	s	Peak period	Yes
N	-	Number of waves	Yes
ρ_w	kg/m³	Water density	No
ν	m²/s	Kinematic viscosity	No
G	m/s²	Acceleration due to gravity	No
A	°	Angle of wave attack: following waves (0°) or opposing waves (180°)	Yes
	-	Spectral shape	No
	-	Groupiness of waves	No

obtained by subtracting the initial bed profile from the bed profile after a test series. The pile, scour protection and sand ripples can be distinguished. The lighter areas indicate erosion (i.e. damage), while the darker areas indicate no change or deposition (of sand or scour protection material). Waves are always travelling from bottom to top.

The three different loading cases (waves only, waves following a current and waves opposing a current) clearly lead to three different damage profiles:

- waves only: Fig. 10 (a) represents a typical wave only case (test 4): damage is present at the sides of the pile, while somewhat smaller erosion is found in front of the pile. The scour protection is damaged up to a distance of approximately 0.5D from the pile. The damage number for the wave alone cases varied between 0.50 (test 82) and 1.67 (test 4), but the same profile was found for all tests. The same damage profile is found in case that a small current is superimposed on the waves, showing that a small steady current does not influence the location of the damage.
- waves following a current: Fig. 10 (b) represents a typical damage profile for waves following a significant current (test 20): damage is mostly found immediately behind the pile and some damage is found at the edges of the pile. In Fig. 10 (b), the test with the largest extension of the damage is shown (test 20). The damage extends over a distance of 1.35D behind the pile and the eroded area is somewhat wider than the pile diameter. In some cases (test 51, 55 and 59), the damage behind the pile is not located immediately behind the pile, but it is located somewhat further from the pile (approximately 0.5D between the pile and the damaged area).
- Wave opposing a current: Fig. 10 (c) represents a typical damage profile for waves opposing a current (test 36): the damage is now located in front of the pile (up to 1D from the pile front, when looking in the travelling direction of the waves). Some damage is also found at the edges of the pile, but never extends further

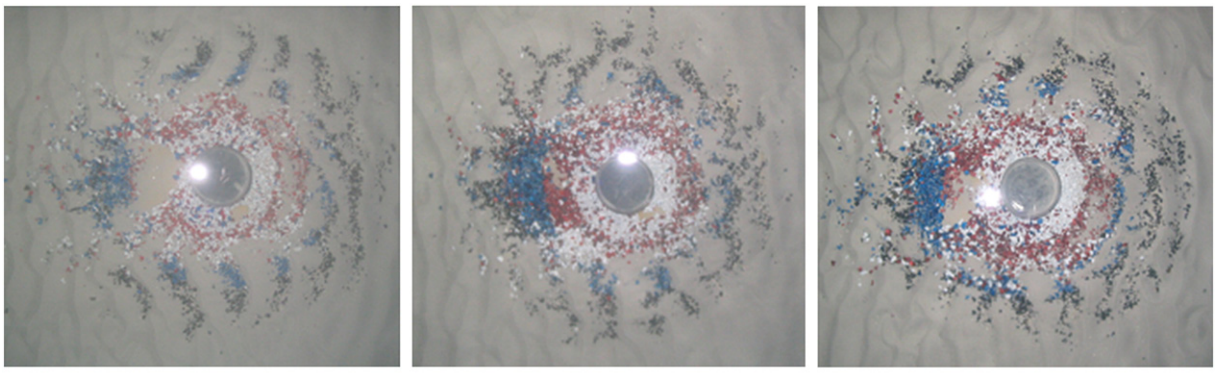

Fig. 8. Damage after 3000 waves for repetitions of test 20; waves and current are travelling from right to left.

Table 4
Structural parameters.

Parameter	Dimension	Description	Variation
D	m	Pile diameter	No
D_{n50}	m	Median stone diameter of scour protection top layer	Yes
D_{85}/D_{15}	-	Ratio of 85% stone diameter to 15% stone diameter of scour protection	Yes
ρ_s	kg/m³	Stone density	Yes
t_s	m	Thickness of armour layer	Yes
E	m	Extension of scour protection	No
Type of foundation	-	Monopile, tripod, gravity based…	No
Construction method	-	Scour protection placed on top of the original bed or placed in a pit	No
		Bed material characteristics	No
Filter type	-	Geotextile, granular filter, no filter	Yes
	-	Shape of stones	No
	-	Mechanical strength of stones	No

than approximately 0.5D from the pile. As for waves following a current, the damaged area in front of the pile is somewhat wider than the pile diameter.

3.2. Prediction formula: damage as a function of the governing parameters

3.2.1. Existing design criteria

Most existing design formulae for a statically stable scour protection give the required stone size as a power function of flow velocity or orbital velocity. Eq. (5) is used in case of a steady current and Eq. (6) in case of waves only (e.g. Chiew, 1995; Soulsby, 1997):

$$D_s = a\frac{U_c^b}{(\Delta g d)^{b/2}} \tag{5}$$

$$D_s = a'\frac{U_w^{b'}}{T^e(g\Delta)^f} \tag{6}$$

with D_s a representative value for the stone size (e.g. the nominal diameter D_{n50}); U_c the steady current velocity; U_w the bottom orbital velocity caused by the waves; g the gravitational acceleration; Δ the relative density of the stones and d the water depth. The constants b and b' which are used as a power of the velocity, are equal to 2 or 3, while the parameter e is approximately equal to 1. The parameter f equals $b'-1$. In the derivation of the design Eq. (9), all parameters, mentioned in Eqs. (5) and (6) have been included.

In the Optipile project (E-Connection et al., 2002–2004), the parameter *Stab* was used to assess the damage level of the scour protection. This parameter is defined as:

$$Stab = \frac{\theta_{\max}}{\theta_{cr}} \tag{7}$$

with θ_{cr} the critical Shields parameter = 0.056 and $\theta_{\max}$ the maximum Shields parameter, defined as:

$$\theta_{\max} = \frac{\tau_{\max}}{\rho_w g(s-1)D_{50}} \tag{8}$$

In the OPTI-PILE project the tests were classified into three damage categories:

- no movement of rocks;
- some movement, but no failure;
- failure.

In De Vos et al. (2011), more details on the OPTI-PILE project are given. The parameter *Stab*, calculated for the tests presented in this paper, is plotted against the visually observed damage in Fig. 11. In den Boon et al. (2004) the limit $Stab = 0.4155$ is defined as the transition between no movement and movement without failure and the limit $Stab = 0.46$ as the transition between movement without failure and failure. Both limits are included in Fig. 11. Although some trend can be observed, it seems that the parameter *Stab* fails to correctly predict the observed damage levels for the present series. In Whitehouse et al. (2006) it was noted that for another test series, the limits for the parameter *Stab* should be adjusted.

A more detailed analysis learns that damage is (sometimes severely) underestimated by the use of the parameter *Stab* for:

- larger current velocities ($U_c > 0.2$ m/s, scale 1/50)
- larger wave periods for the smallest stone size ($T_p = 1.7$ s, scale 1/50)
- smaller wave heights
- high density stones
- opposing currents

The damage is sometimes overestimated for the larger stone sizes, mainly for the peak wave period $T_p = 1.4$ s.

3.2.2. New dynamic design formula

The main goal of the new prediction formula is to include the damage number and to combine the influence of waves and currents into one equation. The number of waves N (i.e. the influence of time

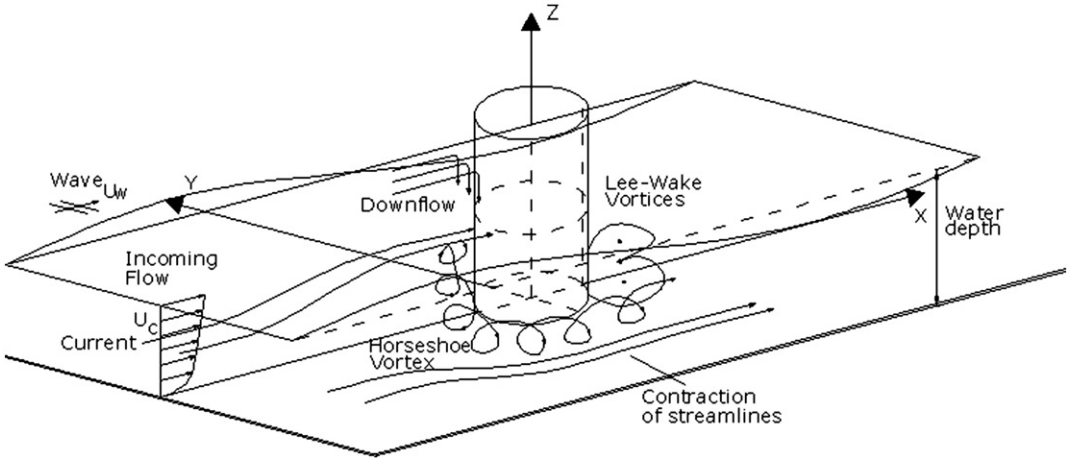

Fig. 9. Definition sketch of the flow–structure interaction for a vertical cylinder.

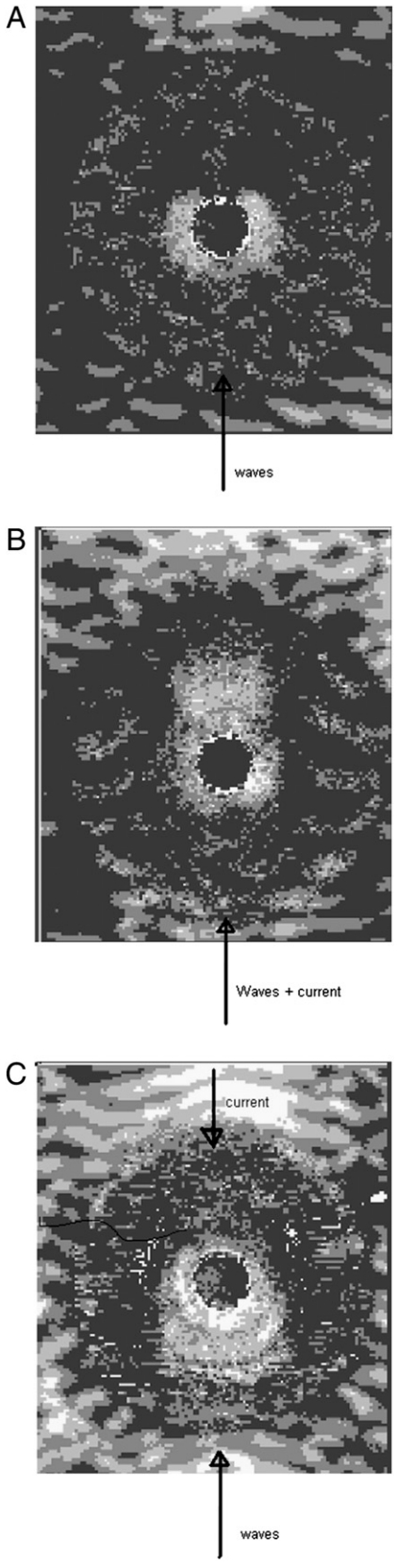

Fig. 10. Location of damage in a scour protection around a vertical pile. Measured elevations [mm] (erosion (<0) and deposition (>0)) from the bed profiles: ■: +20 mm<elevation≤0 mm; ■: 0 mm<elevation≤−5 mm; ■ : −5 mm<elevation≤−10 mm; □: −10 mm<elevation.

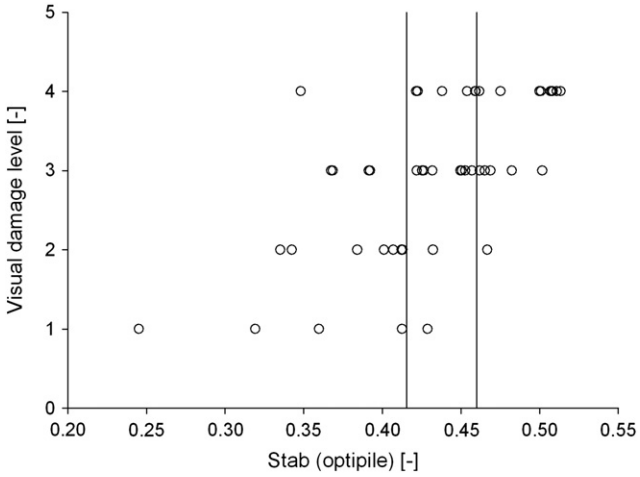

Fig. 11. OPTI-PILE parameter *Stab* (HR Wallingford Ltd for E-Connection Project BV) against observed visual damage level for the present data set.

on the damage development) is also incorporated, as it gives an indication of the development of damage in time.

Eq. (9) is the result of an extensive parameter research and gives an estimate of the damage number S_{3D} (defined in Eq. (4)) as a function of the governing parameters. It is obtained by performing linear regression on the different parameters. The description on the deduction of the formula is given in De Vos (2008). Fig. 12 plots the result of the estimated value of S_{3D}/N^{b0} against the measured value of S_{3D}/N^{b0}.

$$\frac{S_{3D}}{N^{b0}} = a_0 \frac{U_m^3 T_{m-1,0}^2}{\sqrt{gd}(s-1)^{3/2} D_{n50}^2} + a_1 \left(a_2 + a_3 \frac{\left(\frac{U_c}{w_s}\right)^2 (U_c + a_4 U_m)^2 \sqrt{d}}{g D_{n50}^{3/2}} \right) \quad (9)$$

The parameters b_0, a_0, a_2 and a_3 are determined through regression and are respectively equal to 0.243, 0.00076, −0.022 and 0.0079. The parameters a_1 and a_4 depend on the ratio of flow velocity and stone size and on the flow direction and are to be determined as:

$$\begin{aligned} a_1 &= 0 \quad \text{for } \frac{U_c}{\sqrt{g D_{n50}}} < 0.92 \text{ and waves following current} \\ a_1 &= 1 \text{ for } \frac{U_c}{\sqrt{g D_{n50}}} \geq 0.92 \text{ or waves opposing current} \end{aligned} \quad (10)$$

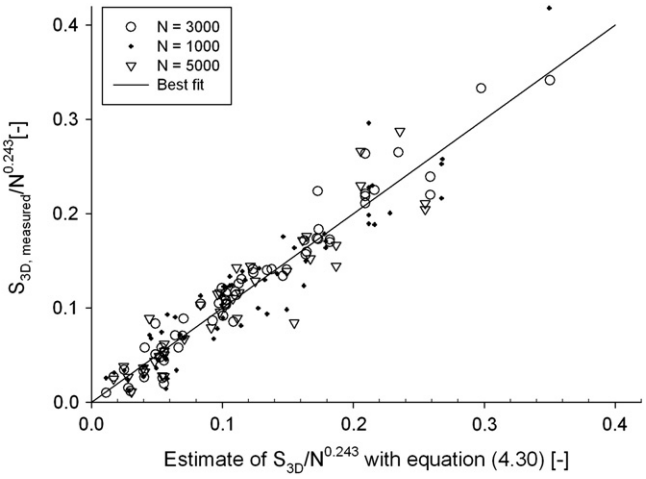

Fig. 12. Measured damage versus estimated damage, using Eq. (9).

$$a_4 = 1 \quad \text{for waves following current}$$
$$a_4 = \frac{Ur}{6.4} \quad \text{for waves opposing current} \tag{11}$$

In Eqs. (9), (10) and (11), U_c represents the depth averaged flow velocity; g is the gravitational acceleration = 9.81 m/s²; D_{n50} the nominal stone diameter, determined from the median stone diameter D_{50} (the stone size for which 50% of the stones is lighter by weight) as:

$$D_{n50}/D_{50} = 0.84 \tag{12}$$

Ur is the Ursell number, often used to describe wave non-linearity (CEM, US Army Corps of Engineers, 2002):

$$Ur = \frac{L^2 H}{d^3} \tag{13}$$

With L the wave length (calculated as for a regular wave with wave height H_{m0} and wave period $T_{m-1,0}$), H the wave height (here the wave height H_{m0} is applied) and d the water depth.

Furthermore, in Eq. (9) N represents the number of waves; d is the water depth; s is the relative density of the stones = ρ_s/ρ_w, with ρ_s = the density of the scour protection material and ρ_w the density of the water; the bottom orbital velocity U_m has to be calculated from the wave spectrum as:

$$U_m = \sqrt{2}\sigma_U \tag{14}$$

with

$$\sigma_U^2 = \int_0^\infty S_U(f)df \tag{15}$$

$$S_U(f) = \left(\frac{2\pi}{T(f)\sinh\left(\frac{2\pi d}{L(f)}\right)}\right)^2 S(f) \tag{16}$$

in which $S(f)$ represents the amplitude spectrum, defined as the ratio of ½ wave amplitude squared and the frequency band width Δf:

$$S(f) = \frac{\frac{1}{2}a^2}{\Delta f} \tag{17}$$

with a the wave amplitude and Δf the frequency band width which depends on the duration of the measurement T_0:

$$\Delta f = \frac{1}{T_0} \tag{18}$$

When the energy spectral wave period $T_{m-1,0}$ is not known, it can be calculated from the wave spectrum as:

$$T_{m-1,0} = T_e = \frac{m_{-1}}{m_0} \tag{19}$$

with the nth moment of the spectral density m_n defined as:

$$m_n = \int_0^\infty f^n S(f)df \tag{20}$$

or, for a JONSWAP spectrum with $\gamma = 3.3$:

$$T_p = 1.107 T_{m-1,0} \tag{21}$$

An iterative approach is needed when the steady flow velocity is sufficiently large to have an influence on the damage development ($U_c/\sqrt{gD_{n50}} > 0.92$), as the fall velocity w_s, used in Eq. (9) depends on the stone size. As a first iteration, it can be assumed that U_c is small, and an initial estimate of the required D_{n50} can be obtained by using the left part of Eq. (9). The fall velocity w_s is then calculated as:

$$w_s = 1.1[(s-1)gD_{50}]^{0.5} \text{ for } D_{50} \geq 1000\ \mu\text{m} \tag{22}$$

When the D_{n50} is known, the D_{50} can be calculated from Eq. (12).

Eq. (9) depends on the flow direction. It was found during the tests that damage was significantly larger for a steady flow opposing the waves, compared to a steady flow following the waves (as is generally used in design model tests). This is described in De Vos (2008).

Eq. (9) can be used to assess which damage number can be expected for an existing scour protection, with a given nominal stone diameter D_{n50} (in this case no iteration is necessary when the steady current velocity is sufficiently large to have an influence on the damage development ($U_c/\sqrt{gD_{n50}} > 0.92$, as the fall velocity can be calculated from the known value of D_{50}).

Eq. (9) can also be used to calculate the required stone size D_{n50} for an acceptable damage number S_{3D}.

3.3. Acceptable damage criterion

It is not immediately clear what can be advised as an acceptable damage level. In fact for a real design the decision on the acceptable damage level should be taken by the designer and owner. In this paragraph, some background information is given.

For a statically stable scour protection, no top layer stones are allowed to move during a design storm, and the scour protection is considered to have failed when the filter is exposed over a minimum area of four armour units $4D_{50}^2$, (den Boon et al., 2004). The same definition is used for failure of the dynamic approach (damage level 4, Section 3.1.1), but limited stone movement of the top layer stones might be accepted during design conditions.

Fig. 5 plots the measured value of S_{3D} against the observed visual damage level (Section 3.1.1). From Fig. 5, it can be deduced that the damage number S_{3D} at which the transition between damage level 3 (movement, but no failure) and damage level 4 (failure) occurs during the test is 1.12. Fig. 13 plots the estimated value of S_{3D}, derived according to Eq. (9) against the observed visual damage level. One could say that for damage numbers higher than 1, the scour protection has failed.

When one considers developing a dynamically stable scour protection, a higher damage number than 1 might be acceptable. In this case, it is very important that damage does not progress over time. The term "failure" which is used to describe damage level 4 is no longer applicable, but a representative profile should be described (Van der Meer, 1988). The damage development during the tests (Fig. 14) indeed leads to the suspicion that such a profile would develop: damage initially develops quite fast and the progression of the damage decreases with the number of waves. However, the geotextile filter is a fixed boundary and does not allow sand to be removed from the exposed area, which means that the maximum damage is achieved when all stones from one sub area are removed. The maximum damage number in this case is equal to the thickness of the scour protection (expressed as times the nominal stone size). When on the other hand no filter or a granular filter is applied, it is likely that bed material will be removed at the location where no armour material is left. This has been investigated by extending some of the tests without filter or a granular filter.

For test 41, in which a granular filter was used, a large current velocity was applied after the last test. The damage number at the end of test 41 (after 5000 waves) was $S_{3D} = 2.39$. A flow velocity $U_c = 0.32$ m/s (water depth $d = 0.2$ m) was maintained during 3 h after test 41 had ended. After this period with a high constant flow velocity, the damage at the side of the pile was found to have increased significantly. Although the damaged area behind the pile

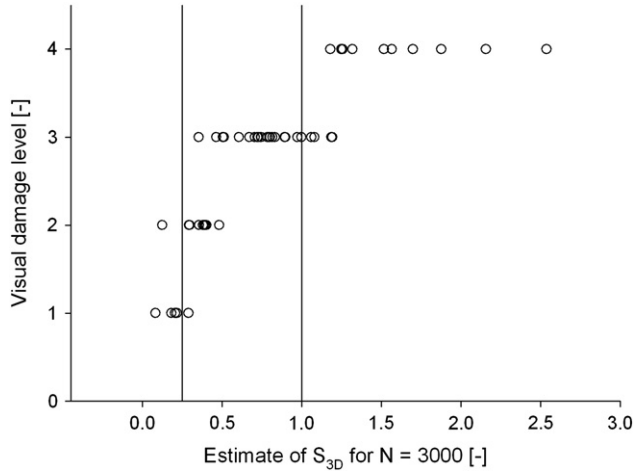

Fig. 13. Estimated damage number (Eq. (9)) versus visual damage level; $N=3000$.

was backfilled during the 3 h test with large steady current, a significant scour hole developed beside the pile. The depth of the scour hole was approximately 3 cm deep, leading to a value of $S/D=0.3$. The damage after the high flow velocity increased from $S_{3D}=2.39$ up to $S_{3D}=3.25$.

Also test 38, in which no filter was used, was extended with an additional test to investigate the stability of the developed profile. The damage number at the end of test 38* was $S_{3D}=1.70$. First a flow velocity of 0.28 m/s was applied. This did not alter the developed profile. When waves were added to the maintained steady current velocity of 0.28 m/s, a significant scour hole developed both in front of and beside the pile (significant wave height $H_{m0}=0.12$ m and peak wave period $T_p=1.7$ s, duration 500 waves). Fig. 15 shows the measured sections parallel with the flow (bottom) and perpendicular to the flow (top) which go through the point with maximum scour depth. The initial profile, the final profile and the profile after the additional test are plotted, showing clearly that scour occurred because the scour protection was damaged. The damage after 500 additional waves increased from $S_{3D}=1.70$ (damage number after 5000 waves) up to $S_{3D}=5.23$.

A high flow velocity ($U_c=0.3$ m/s) was also imposed on the scour protection after test 37, in which no filter was placed between the armour layer and the sand. The damage which was measured after 5000 waves $S_{3D}=1.1$. Visually, no difference could be seen before and after the high flow velocity was applied (no clear scour pattern

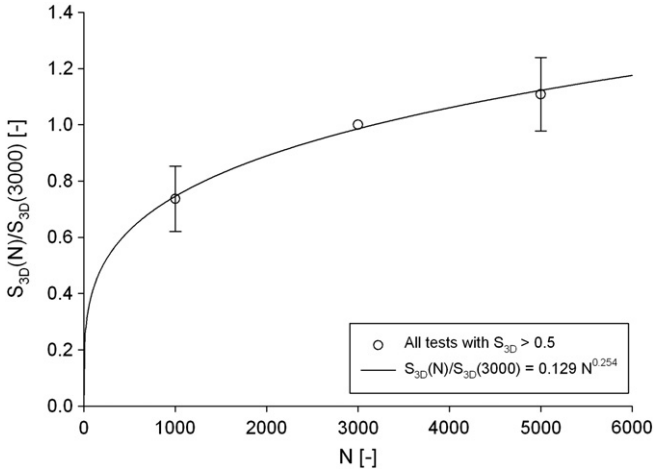

Fig. 14. Influence of number of waves on damage number.

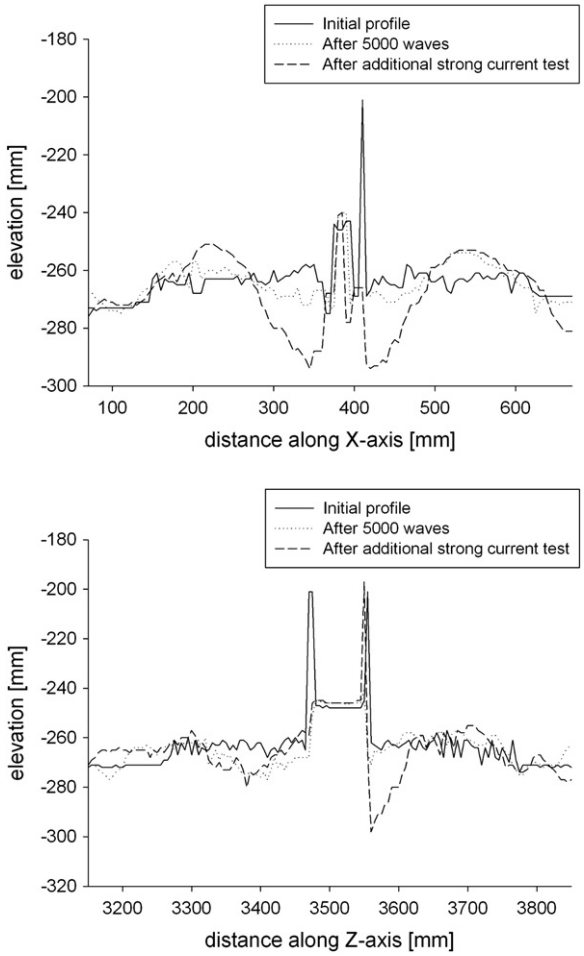

Fig. 15. Cross-sectional plane for test 38 (initial profile, profile after 5000 waves and profile after additional test). top: perpendicular to the flow, bottom: parallel with the flow.

developed). The profile was therefore not measured after the high flow velocity.

The tests described earlier show that for large current velocities (and small wave heights), damage increases and a scour hole develops when the armour layer has initially failed. It was found that this situation is not acceptable, as it could lead to the failure of the scour protection. It is therefore advised not to design for a damage level "4" and the development of a dynamically stable profile is not possible for the applied scour protection with thickness $2.5D_{n50}$.

The development of a dynamically stable profile might be possible when a thicker scour protection armour layer is used and when the filter or bed material is not exposed during the storm. This topic requires more research before any conclusions can be drawn.

Again, what is an acceptable damage level for a scour protection should be decided by the designer of the scour protection. To help the designer, the top view pictures of all test results (after 3000 waves) are added in Appendix A.

3.4. Influence of filter type

A geotextile filter was used throughout most of the tests. Even though the aim of this test series was not to investigate filter design, the alternative of using no filter or a granular filter was tested. Fig. 16 shows the influence of the filter type on the damage. As could be expected, the difference in damage number for tests with or without filter and a small damage number lies within the accuracy range and therefore does not differ significantly. This was expected, as the filter

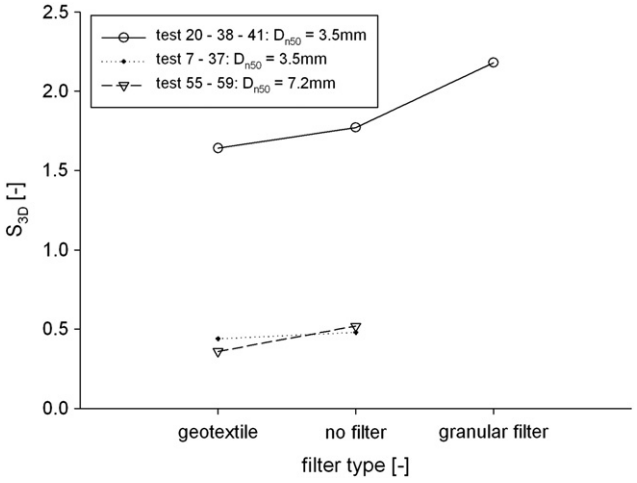

Fig. 16. Influence of filter type on damage number.

avoids bed material to be transported. No bed material is lost through the armour layer in case no filter is used, but this might be due to scaling problems and might not represent the prototype situation. This means that for the model tests, bed material will only be transported once the armour layer disappears and therefore the filter type does not influence the damage for small amounts of damage.

A significant increase in the damage number is found for test 41, in which a granular filter was applied. The increase in damage number is most likely caused by the higher location of the armour material above the bed, as the filter, which was placed on top of the bed, had a thickness of 1 cm. The higher location increases the disturbance of the flow and brings on higher orbital velocities at the top off the scour protection. The increase in damage is also caused by the loss of bed material at the location where the filter (and even bed material) is exposed.

3.5. Further research

The test series was quite extensive. However, there are a few parameters which haven't been or have been insufficiently tested and are therefore not included in Eq. (9). These parameters are:

- filter type: for high damage numbers, damage is significantly larger in case no filter or a granular filter is used. When only limited damage is allowed for, the filter type probably has little influence on the expected damage level. However, further investigation on the influence of different filter types on the damage number should confirm this hypothesis;
- construction type of scour protection: damage might be influenced by the protrusion of the scour protection above the bed;
- pile diameter: only one pile diameter was tested. The result is therefore only valid for pile diameters which do not vary too much from the tested pile size. As the pile diameter has an influence on the vortex shedding, it is likely that it will have an influence on the damage number; as the size of the subzones depends on the pile diameter, this influence might be small.
- foundation type: other foundations, such as tripods or gravity based foundations have a different influence on the flow pattern. It is to be expected that the damage development will be influenced by the foundation type.
- damage due to steady current alone: no tests were performed with flow velocities which are high enough to move the stones. Some expressions exist to calculate the required stone size for a statically stable stone size, but extra model tests are needed to include the damage number.

Table 5
Comparison between required stone size (D_{50} [m]) according to different traditional calculation methods for different values of the amplification factor: $d=20$ m; $H_{m0}=6.5$ m; $T_p=11.2$ s; $U_c=1.5$ m/s; $D_{85}/D_{15}=2.5$.

Amplification α	Traditional approach according to Fredsoe and Deigaard, use of τ_m	Traditional approach according to Soulsby, use of τ_{max}	Soulsby (1997), Waves	Soulsby (1997), current	De Vos, Static approach
2	0.68	0.66	0.29	0.013	0.496
3	1.30	1.51	0.55	0.022	0.496
4	1.97	2.75	0.85	0.033	0.496

Further research is required to assess to what extent these parameters influence the damage number. Furthermore, more research is required to assess the influence of a reverse current, the influence of water depth and large flow velocities on the damage development.

4. Application of the new prediction formula

In this section, the required stone size for a scour protection around a monopile foundation and a typical situation in the North Sea is calculated with different methods. The methods which are used are the same as the ones used in part 1 (De Vos et al, 2011) and the formulas which were used are described in part 1:

- the traditional approach, in which the amplified combined current and wave bed shear-stress determine the critical bed shear-stress. The amplification factor α for the bed shear stress is varied (value of $\alpha=2$, 3 and 4) to account for the influence of the pile. Two approaches are used to calculate the bed shear stress. The first method is the method according to Fredsøe and Deigaard (1992), the second method is the one according to Soulsby (1997).
- the static prediction formula, derived in part 1 (De Vos et al., 2011).
- The equations given by Soulsby (1997), which calculate a critical stone size for the two separate loading conditions: wave loading and steady flow. No interaction between waves and current is considered. Again, the amplification factor α for the bed shear stress is varied (value of $\alpha=2$, 3 and 4) to account for the influence of the pile, both for the steady flow as for the wave induced flow velocity.
- the dynamic prediction formula, given by Eq. (9). The damage level S_{3D} was given a value of 0.2, 0.5 and 1, both for waves following and opposing a current.

The OPTI-PILE parameter's calculation is bound to confidentiality and can therefore not be included in this calculation.

The example is characterised by the following parameters:

A monopile foundation is to be installed in a water depth of 20 m. The pile diameter is 5 m. The design wave conditions have a significant wave height $H_{m0}=6.5$ m. The corresponding peak wave period $T_p=4.4\sqrt{H_{m0}}=11.2$ s. The tidal velocity has an average value $U_c=1.5$ m/s. D_{85}/D_{15} is assumed to be equal to 2.5. In Table 5, the comparison is made between the required scour protection stone sizes for the calculation methods resulting in a statically stable scour protection. Table 6 gives

Table 6
Comparison between required stone size (D_{50} [m]) according to the static approach and the dynamic approach, for different values of acceptable damage number S_{3D}: $d=20$ m; $H_{m0}=6.5$ m; $T_p=11.2$ s; $U_c=1.5$ m/s; $D_{85}/D_{15}=2.5$.

Accepted damage level S_{3D}	De Vos, dynamic approach, waves following current	De Vos, dynamic approach, waves opposing current
0.2	0.44	0.46
0.5	0.32	0.36
1	0.27	0.28

the results for the required stone size when using Eq. (9) for different values of S_{3D}. It shows that, for this example, the stone size is only slightly smaller than the stone size obtained with the static approach from part 1 when using a very small value of the accepted damage level (e.g. $S_{3D}=0.2$). A significantly smaller stone size can be obtained when using Eq. (9) and allowing a somewhat higher amount of damage (S_{3D} between 0.5 and 1). For this example a reduction factor between 1.2 and 1.8 is obtained. As mentioned, a slightly larger stone size is required when applying a reverse current.

5. Conclusion

In this paper, the experimental research which was performed to determine the required stone size for the top layer of a scour protection around a monopile foundation in a combined wave–current climate is discussed. A dynamic design approach is used, leading to a scour protection for which limited movement of top layer stones during a design storm might be accepted.

The experiments were performed with irregular waves and a steady current on a scale 1/50. Design Eq. (9) gives the required stone size as a function of the accepted damage number. It was found that damage is higher for a steady current opposing the waves, and that the damage profile mainly depends on the direction and presence of the steady current. Furthermore, some tests were carried out to verify whether a dynamically stable profile develops for large damage numbers. This did not seem to be the case. It is therefore advised to design for a limited accepted damage level, when applying a scour protection with a limited thickness (e.g. $2.5D_{n50}$, which was also applied during the tests).

When comparing the proposed design formula to the existing design methods, and with the static approach, described in part 1, a significant reduction in required stone size can be achieved when allowing a damage number S_{3D} up to 1.

It is advised to compare the results obtained with Eq. (9) with other data sets or field measurements when possible.

Acknowledgements

The authors gratefully acknowledge the Research Foundation — Flanders for the grant which was provided for their research at Ghent University.

Appendix A. Pictures of dynamic scour protection tests

In this appendix, pictures of the top view of all scour protection tests with irregular waves are shown below. The pictures after 1000 waves, 3000 waves and 5000 waves are shown. The tests are shown in order of the measured damage. The damage after 3000 waves (in volume % of eroded material) is included, as is the test number. The test matrix is given in the main text (Table 1). Waves are always travelling from right to left. The direction of the steady current is indicated with an arrow.

References

Breusers, H.N.C., Raudkivi, A.J., 1991. Scouring-hydraulic Structures Design Manual. IAHR, A.A. Balkema, Rotterdam. p. 143.
CEM, US Army Corps of Engineers, 2002. Coastal Engineering Manual 1110-2-1100, Washington, D.C.
Chiew, Y.M., 1995. Mechanics of riprap failure at bridge piers. Journal of Hydraulic Engineering 121 (9), 635–643.
CIRIA/CUR, 1991. Manual on the use of rock in coastal and shoreline engineering. CIRIA/CUR special publication, 83, p. 607.
den Boon, H., Hessels, J., van Rooij, J., 2003. Cost reduction of offshore wind parks by low cost load monitoring of pile foundations, offshore wind energy in Mediterranean and other European Seas (OWEMES), Napels, Italy.
den Boon, J.H., Sutherland, J., Whitehouse, R., Soulsby, R., Stam, C.J.M., Verhoeven, K., Høgedal, M., Hald, T., 2004. Scour behaviour and scour protection for monopile foundations of offshore wind turbines. European Wind Energy Conference & exhibition (EWEC), London, UK.
De Vos, L., 2008. Optimisation of scour protection design for monopiles and quantification of wave run-up. Engineering the influence of an offshore wind turbine on local flow conditions. PhD Thesis, Ghent University, Ghent, pp 319.
De Vos, L., De Rouck, J., Troch, P., Frigaard, P., 2011. Empirical design of scour protections around monopile foundations. Part 1: Static Aproach, Coastal Engineering, 58. Elsevier.
E-Connection, Vestas Wind Systems D.K., Germanischer Lloyd Windenergie D., 2002–2004. OPTI-PILE, Fifth Research and Technological Development Framework Programme.
Federal Highway Administration, 2008. Use of Waste and Byproduct Materials in Pavement Construction.
Fredsøe, J., Deigaard, R., 1992. Mechanics of Coastal Sediment Transport. Advanced Series on Ocean Engineering, Vol. 3. World Scientific.
Redeker, F., 1985. Probabilistic Approach of Cover Layer Material. Delft University of Technology.
Soulsby, R., 1997. Dynamics of Marine Sands: a Manual for Practical Applications. Thomas Telford.
Sumer, B.M., Fredsøe, J., 2002. The mechanics of scour in the marine environment. Advanced Series on Ocean Engineering. World Scientific, River Edge, N.J. 536pp.
Whitehouse, R.J.S., Sutherland, J., O'Brien, D., 2006. Seabed scour assessment for offshore windfarm, International Conference on scour and erosion, Nanyang University, Nanyang, Singapore.
Van der Meer, J.W., 1988. Rock Slopes and Gravel Beaches Under Wave Attack. Delft Hydraulics.